


## Cell response to PLA scaffolds functionalized with various seaweed polysaccharides

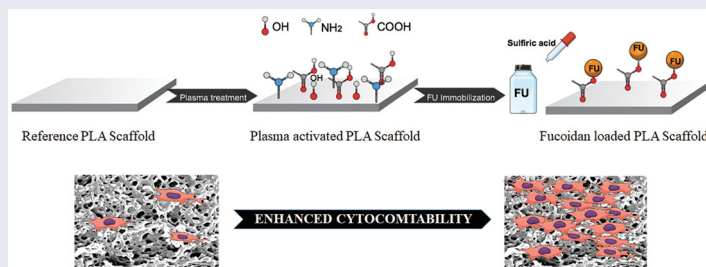
Kadir Ozaltin<sup>a</sup> , Elif Vargun<sup>a,b</sup>, Antonio Di Martino<sup>a,c</sup>, Zdenka Capakova<sup>a</sup>, Marian Lehocky<sup>a</sup>, Petr Humpolicek<sup>a</sup>, Natalia Kazantseva<sup>a</sup>, and Petr Saha<sup>a</sup>

<sup>a</sup>Centre of Polymer Systems, Tomas Bata University in Zlín, Zlín, Czech Republic; <sup>b</sup>Faculty of Science, Chemistry Department, Mugla Sıtkı Kocman University, Mugla, Turkey; <sup>c</sup>Research School of Chemistry and Applied Biomedical Sciences, Tomsk Polytechnic University, Tomsk, Russian Federation

### ABSTRACT

The porous polylactic acid matrix has been particularly developed as a scaffold in tissue engineering, drug loading, and wound dressing. However, the loading of active chemical compounds is challenging due to its highly hydrophobic nature and lack of functional groups for chemical bonding. Plasma treatment is a fast, heat and chemical-free solution to increase its hydrophilicity by oxidative functional groups and physical etching. In this study, a highly porous PLA scaffold was obtained by polyethylene glycol pore formation agent and treated by radiofrequency (RF) air plasma. Fucoïdan from *Fucus vesiculosus*, *Macrocystis pyrifera*, and *Undaria pinnatifida* were used to immobilize onto the activated porous PLA surface for use as medicated wound dressings. The chemical composition and morphology were investigated by FTIR, SEM-EDS analysis, and cytocompatibility assay was studied mouse embryonic fibroblast cells (NIH/3T3).

### GRAPHICAL ABSTRACT



### ARTICLE HISTORY

Received 9 April 2020  
Accepted 16 July 2020

### KEYWORDS

Poly(lactic acid); fucoïdan; PLA scaffold; fibroblast cell; plasma treatment

## 1. Introduction

Poly(lactic acid) (PLA) is an aliphatic polyester belonging to the  $\alpha$ -hydroxyl acid family. It is obtained from lactic acid by direct polycondensation or by ring-opening polymerization of the lactide dimer. The biodegradable and biocompatible nature of the PLA offers various practical applications such as medical implants, drug delivery, cosmetics, and food packaging<sup>[1]</sup>. The porous PLA matrix has been developed as a scaffold in tissue engineering, drug loading, and wound dressing<sup>[2–4]</sup>.

There are several techniques to fabricate a porous PLA matrix for special applications such as solution casting/pore leaching, electro-spinning, emulsion freeze drying, gas foaming, and phase inversion<sup>[5–8]</sup>. Each method possesses advantages and disadvantages and should meet the specified demands. Among these techniques, the solution casting/pore leaching method is easy to control the porosity. The ability to control the porosity and pore size plays a

crucial role in the biomaterials used as a scaffold for wound dressing applications. The introduction of pores can enhance cell migration, cell proliferation, and regulate the tissue integration. The morphology of the porous biomaterials (pore size/shape, pore interconnectivity) has been regulated by controlling the amount and dimension of porogen particles<sup>[9]</sup>. Chitrattha and Phaechamud<sup>[10]</sup> explained that the porous architecture of wound dressing can reduce the contact area with the soft tissue to avoid adherence when the wound is dried.

Toughness and elasticity are desired mechanical properties of biomaterials used for the soft tissues. However, PLA is characterized by its high tensile strength, rigidity, and hydrophobicity. To eliminate these drawbacks, different methods such as copolymerization with other monomers or blending with hydrophilic polymers are employed. Diblock copolymers of PLA and poly(ethylene glycol)-monomethyl ether were investigated as drug and cell carriers<sup>[11]</sup>. PLA-b-poly(ethylene glycol) amphiphilic block copolymer composite

scaffold was studied as a hydrophilic drug carrier and found a better dispersion property and stabilized the release of hydrophilic drugs<sup>[12]</sup>. To improve the ductility and toughness of PLA, it was blended with polyamide and poly( $\epsilon$ -caprolactone) and thermoplastic starch<sup>[13,14]</sup>. These methods are successful in enhancing the hydrophilicity and improving the toughness. However, the main problem with these techniques is that the modification of the entire bulk material can result in the loss of some desired properties of the pure PLA such as mechanical strength and degradation stability. Hence, surface modification techniques have been used to change the polymer surfaces properties without sacrificing mechanical and/or structural properties. Plasma treatment is a unique technique to change various surface properties, especially wettability and surface roughness. The hydrophilic surfaces can be obtained by incorporating hydrophilic oxidative functional groups, e.g. carboxyl ( $-C-O-O-H$ ), carbonyl ( $-C=O$ ) and hydroxyl ( $-OH$ ) upon air plasma treatment. It has been known that the hydrophilic surface of biomaterials has a significant influence on cell attachment or proliferation and also serves as a hydrophilic drug carrier<sup>[15,16]</sup>. The two-step plasma treatment to provide the oxygen- and nitrogen-containing functional groups onto honeycomb pattern on PLA film and the treatment had a major impact on cytocompatibility determined by NIH/3T3 fibroblasts<sup>[17]</sup>. Plasma treatment of PLA film provided not only increased oxygen content and wettability but also increased the initial cell attachment both quantitatively and qualitatively<sup>[18]</sup>. Surface chemistry of PLA-type copolymers e.g., di- and tri-block copolymers of PLA-PEG were also altered by plasma treatment<sup>[19]</sup>. The results of cell culture experiments showed that the cell affinity of the PLA surface after a combination of plasma treatment and collagen anchorage was greatly improved. Stloukal et al.<sup>[20]</sup> investigated the effect of plasma treatment on the release kinetics of the drug Temozolomide (TMZ) from PLA and PLA-polyester urethane polymer blend film. The rate of release over the initial 24 h slowed down several times which means in a more controlled manner.

Fucoidan is one of the promising polysaccharides to immobilize materials surface to obtain active biomaterials in soft tissue engineering. Fucoidans are a sulfated ester, fucose-rich (L-fucopyranose units) biopolymers found in brown macroalgae<sup>[21]</sup>. These algae derived marine carbohydrate polymers were examined for potential bioactivities including antitumor, antiviral, antithrombotic, and anticoagulant activities<sup>[22–27]</sup>. The high degree of sulfation, structure, and molecular weight of fucoidans determine these prominent biological activities<sup>[28]</sup>. Recently, researches have shown that the fucoidan containing biomaterials serves as a carrier for hydrophilic drugs/biofactors especially in the fields of cancer, regenerative medicine, and cardiovascular diseases<sup>[29]</sup>.

Our previous studies, coating the polyethylene terephthalate surface, to use in blood-contacting applications, by fucoidan from *Fucus vesiculosus* via plasma treatment demonstrated high anticoagulation properties<sup>[30,31]</sup>. In this study, three different types of fucoidan were loaded to

highly porous and plasma-treated PLA scaffold to create a biodegradable artificial extracellular matrix with an enhanced cell adhesion/proliferation performance. PEG was used as a porogen with a 75% mass ratio to obtain highly porous PLA scaffold to enhance its cell interactions in 3D and increased surface area, proportional to pores, to load more amount of fucoidan particles. Furthermore, the thickness of the PLA scaffold was set to 25  $\mu$ m to accelerate its degradation rate/time in the body after the release of fucoidan and fibroblast cells create their natural extracellular matrix instead of the artificial PLA scaffold. Such scaffolds can be produced with various biopolymers and methods for both soft and hard tissue applications<sup>[32–39]</sup>.

## 2. Experimental

### 2.1. Materials

The pellet form of poly(lactic acid) (PLA) 4032D was purchased from Nature Works (Blair, NE). Poly(ethylene glycol) (PEG) with a molecular weight of 4000 and dichloromethane (99.8%) were purchased from Sigma-Aldrich. Polysaccharides of fucoidan from *Fucus vesiculosus*, fucoidan from *Macrocystis pyrifera*, and fucoidan from *Undaria pinnatifida* were purchased from Sigma-Aldrich.

### 2.2. Preparation of the highly porous PLA scaffold

The highly porous PLA scaffold was prepared by solution casting/porogen leaching technique, using PEG as a porogen. The weight ratio of PLA:PEG was 25:75. The PLA and PEG were dissolved in dichloromethane and the solution concentration was 143 g/L. The viscous solution was poured onto the clean glass plate and spread by the doctor-blade method to obtain PLA/PEG films with a thickness of 25  $\mu$ m. Subsequently, the PLA/PEG films were placed into deionized water for 48 h (water refreshed every 12 h) at room temperature (RT) to leach out PEG and obtain highly porous PLA scaffold with interconnected pore structure. The final products of porous PLA scaffolds were dried in an oven for 12 h at 50 °C and referred to as PLA-REF thereafter.

### 2.3. Loading of the fucoidans to the scaffold

Aqueous solutions of 0.1% (w/v) of fucoidans were prepared and the pH of the solutions were set to 5 with the addition of  $H_2SO_4$  and placed in solution vials. Dried PLA-REF scaffolds were subjected to radio frequency (RF) air plasma at 50 W of reactor power and 13.56 MHz frequency, generated by a PICO (Diener, Germany) plasma reactor for 60 s. This was to activate their surface by plasma treatment for enhancing the chemical interactions with active groups of fucoidan. Air was used with a 20 sccm flow rate as a discharge gas under the chamber pressure of 50 Pa. Immediately after the plasma treatment, the scaffolds were placed into each vial containing aqueous solutions of fucoidan from *Fucus vesiculosus*, fucoidan from *Macrocystis pyrifera*, and fucoidan from *Undaria pinnatifida* for 24 h at

RT on a shaker. Finally, the scaffolds were washed gently in distilled water and dried at RT overnight. The plasma-activated sample referred to as PLA-RF and fucoidan loaded scaffolds referred to as PLA-RF-FV, PLA-RF-MP, and PLA-RF-UP, thereafter.

#### 2.4. The scaffold morphology and elemental analysis by scanning electron microscope

The morphology of the scaffold was monitored by a NANOSEM 450 (FEI, Hillsboro, USA) scanning electron microscope (SEM) equipped with an energy dispersive X-ray spectroscopy (EDS) analyzer. SEM operated at 5 kV under 90 Pa pressure in a water vapor environment to reveal pore size and its distribution for the morphology investigation. Before analysis, samples were frozen by liquid nitrogen to maintain the porous structure and then broken into two parts to reveal their lateral section. Images were taken at the various magnifications of 5 k $\times$  and 20 k $\times$  with a spot size of 50 nm. Elemental analysis was carried out by a high sensitivity Circular Backscatter Detector (CBS) operated at 15 kV with a spot size of 4.5.

#### 2.5. Ftir analysis

The changes in chemical compositions of the PLA scaffolds were examined by a Nicolet iS5 (Thermo Scientific, Grand Island, NY) single beam Fourier transform infrared spectroscopy (FTIR) equipped with iD5 attenuated total reflectance (ATR). The FTIR spectrum was recorded between 400 and 4000  $\text{cm}^{-1}$  with a resolution of 2  $\text{cm}^{-1}$  and 64 scans using a ZnSe crystal at an incident angle of 45 $^\circ$ .

#### 2.6. Water contact angle measurement

Surface wettability behavior of the PLA scaffolds was carried out by the Sessile drop method via the SEE System (Advex Instruments, Brno, Czech Republic) equipped with a CCD camera, to determine their surface hydrophilicity. Ten separate droplets of distilled water with a volume of 5  $\mu\text{L}$  were placed onto each sample surface at 23  $^\circ\text{C}$  and 63% relative humidity, to obtain mean water contact angle value (Qw).

#### 2.7. Cell proliferation assay

The cytocompatibility was determined *in vitro* using mouse embryonic fibroblast cells (NIH/3T3, ATCC<sup>®</sup> CRL-1658<sup>™</sup>, USA). This cell line is one of the most used cell lines within the initial testing of materials cytocompatibility. The samples for cytocompatibility testing were prepared with a dimension of 10  $\times$  10 mm in the form of thin foil. Previous to testing, the specimens were disinfected with a UV radiation with wavelength of 258 nm for 30 min on each side. The ATCC-formulated Dulbecco's Modified Eagle's Medium (BioSera, France) containing 10% of calf serum (BioSera, France) and 100 U  $\text{mL}^{-1}$  Penicillin/Streptomycin (BioSera, France) was used as a cultivation medium. The cells were seeded onto the samples in concentrations of  $2 \times 10^4$  cells

per  $\text{mm}^2$  and incubated for 72 h at 37  $^\circ\text{C}$ . After the incubation period, cell proliferation was evaluated in two ways: (1) qualitative by observation of morphology and (2) quantitative by MTT assay.

For the cell morphology, cells were fixed with 4% formaldehyde (Penta, Czech Republic) for 15 min, then rinsed by phosphate-buffered saline (PBS, Invitrogen). Subsequently, the aqueous solution of nonionic surfactant 0.5% Triton X-100 (Sigma-Aldrich) was applied for 5 min to permeabilized the cells. After permeabilization, the cells were washed by PBS three times then a drop of ActinRed<sup>™</sup> 555 (Thermo Fisher Scientific, USA) with 10  $\mu\text{g mL}^{-1}$  Hoechst 33258 (Invitrogen, USA) were added in the required amount of PBS and left to incubate for 30 min in the dark to stain the cell cytoskeleton and nuclei. Finally, cell proliferation and morphology were observed by a fluorescent inverted Olympus phase contrast microscope (IX 81, Japan). All the tests were performed three times.

For the quantification of viable cells, the MTT solution was added to each sample in concentration 0.5  $\text{mg mL}^{-1}$ . The cells were incubated with the MTT solution for 4 h. Afterwards, resulting formazan was dissolved in DMSO and the absorbance was measured at 570 nm on Infinite M200 PRO (Tecan, Switzerland). All the tests were performed in quadruplicates. The cell viability is expressed as relative percentage compared to the reference sample (PLA-REF), which was adjusted as 100%.

### 3. Results and discussion

#### 3.1. The scaffold morphology analysis

The morphology of the porous PLA scaffold prepared with 75% of pores was investigated by SEM (Figure 1). The total thickness of the scaffold is measured as 25  $\mu\text{m}$  with a pore size ranging from 500 nm to 10  $\mu\text{m}$ . The highly porous structure provides the condition for 3D cell growth, instead of limited 2D surface area, by increased pore size during the time of degradation. Furthermore, due to the increased surface area by pores, the amount of the loaded fucoidan and its effect expected to be higher. Besides the effect on 3D cell growth, the PLA degradation is enhanced due to its thin and highly porous structure, which resembles the natural extracellular matrix.

#### 3.2. Sem energy dispersive spectroscopy results

The chemical compositions of the fucose containing polysaccharide fucoidans-loaded porous PLA scaffolds were evaluated by using a scanning electron microscope equipped with energy dispersive spectroscopy (EDS), and the results are listed in Table 1. The reference porous PLA sample (PLA-REF) has a content of carbon and oxygen with the levels of 59.48 and 40.42%, respectively. After RF plasma treatment, the oxygen level slightly increased to 41.92 and 2.14% of nitrogen was detected, due to functional groups introduced by plasma particles and the carbon level decreased to 55.94%, correspondingly. The success in the



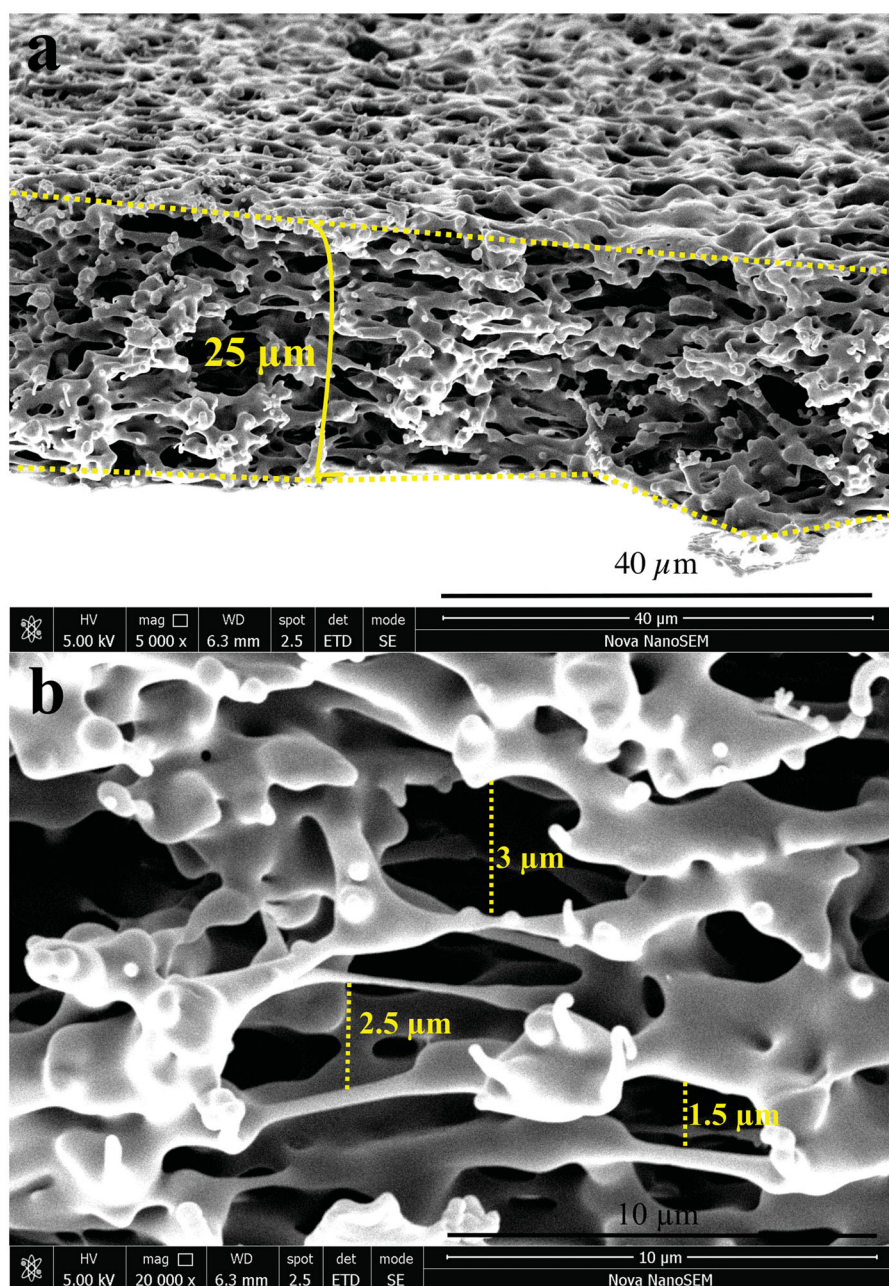


**Figure 1.** The morphology of the PLA-REF porous scaffold, investigated by SEM. (a) Surface with lateral section. (b) Lateral section.

**Table 1.** Elemental analysis results by SEM-EDS.

Samples	C	O	N	S
PLA-REF	59.48	40.42	–	–
PLA-RF	55.94	41.92	2.14	–
PLA-RF-FV	54.88	43.44	1.21	0.48
PLA-RF-MP	55.56	42.64	1.26	0.54
PLA-RF-UP	54.99	43.12	1.6	0.29

immobilization process is proven with the presence of sulfur groups belonging to fucoidan. As is seen in [Table 1](#), each of the fucoidans-loaded samples displayed sulfur content. Among those, the maximum sulfur content observed was PLA-RF-MP with a level of 0.58%, followed by PLA-RF-FV with a level of 0.48%, and lowest was PLA-RF-UP with a level of 0.29%. Therefore, the highest cell proliferation activity is expected for PLA-RF-FV and PLA-RF-MP samples

due to their higher sulfur content as an indicator of the level of immobilized fucoidan species.

### 3.3. ATR-FTIR analysis results

The ATR-FTIR spectra of the porous PLA scaffolds are presented in [Figure 2](#). The characteristic peaks of PLA were identified in a control scaffold and no obvious peaks for PEG were observed in the spectrum. This means that PEG porogen was removed from PLA matrix completely. The FTIR spectrum of PLA (control) sample revealed that the asymmetric and symmetric  $-\text{CH}$  stretching in  $-\text{CH}_3$  group appeared at  $2996\text{ cm}^{-1}$  and  $2942\text{ cm}^{-1}$ , respectively. The intense peak at  $1749\text{ cm}^{-1}$  is attributed to the  $\text{C}=\text{O}$  bond stretching. The peaks at  $1456\text{ cm}^{-1}$  and  $1364\text{ cm}^{-1}$  correspond to the asymmetric and symmetric  $-\text{CH}$  bending in

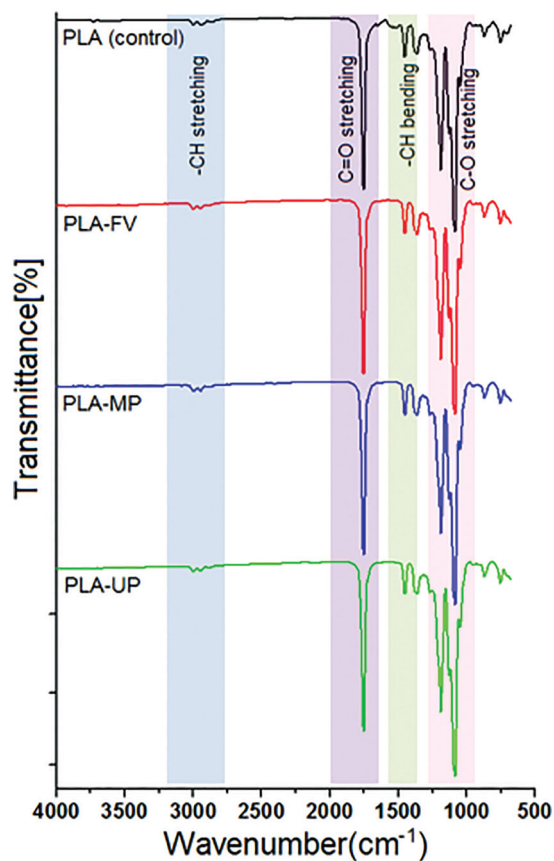


Figure 2. ATR-FTIR spectra of the porous PLA scaffold and three fucoidans-loaded PLA scaffolds.

-CH<sub>3</sub> group, respectively. The stretching peaks of C-O and C-O-C bonds were identified at 1187 cm<sup>-1</sup> and 1087 cm<sup>-1</sup>, respectively. The observed peaks of all samples correspond to PLA and agree well with data in the literature<sup>[40,41]</sup>. The lack of -OH stretching peak at 3400 cm<sup>-1</sup>, corresponds to PEG, indicates leaching PEG from the structure. The spectra related to the fucoidan loaded scaffolds present the same absorption peaks as REF-PLA. This indicates that the immobilization of fucoidan was achieved at an atomic level on the surface of the porous PLA scaffold.

### 3.4. Water contact angle results

Surface hydrophilicity of the porous PLA scaffolds was performed by the water contact angle test and results are given in Figure 3. The highly hydrophobic nature of PLA-REF sample was monitored with a water contact angle value of 82.3°, in spite of its highly porous structure. This highly hydrophobic nature and lack of free functional groups inhibit chemical agent immobilization onto the PLA-REF surface. After RF plasma treatment, the water contact angle value drastically decreased to 58.3° for the sample PLA-RF. This increase in hydrophilicity is due to the increased surface area by plasma etching and also hydrophilic oxidative functional groups introduced by plasma particles. Therefore, the immobilization of anticoagulant agents is possible by chemical bonding with created functional groups, moreover, it is possible to load more agents due to increased surface

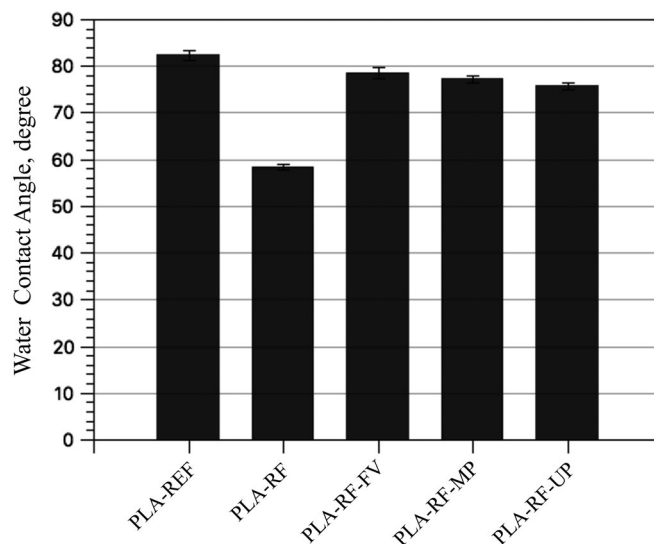


Figure 3. Water contact angle ( $\theta^\circ$ ) values of the samples.

area. As it can be seen in Figure 3, anticoagulant fucoidan immobilized samples of PLA-RF-FV, PLA-RF-MP, and PLA-RF-UP demonstrated similar water contact angle values within a range of 75.7°–78.5°. This indicates successful immobilization of each anticoagulant fucoidan after plasma treatment by increasing the water contact angle value due to their hydrophilic nature and the filling of the etched surface area.

### 3.5. Cell proliferation on the scaffolds

Plasma techniques have made changes in surface chemical composition and topography that affect cell behavior<sup>[42]</sup>. To control cell adhesion and proliferation, it is vital not only having specific functional groups on the surface but also possessing optimum surface topography<sup>[43]</sup>. An *in vitro* cytocompatibility test was performed using mouse embryonic fibroblast (NIH/3T3) cells and results are given in Figure 4. As can be seen in Figure 4, on the porous PLA scaffold, without any modification, viable cells are observed. However, the quantity of cells is lower than that of fucoidan loaded counterparts and the cell morphology is slightly different. On the PLA-REF sample, the typical fibroblast branching is missing. This was likely caused due to the lack of active compounds to enhance cell attachment and growth. Apart from the chemical composition of the scaffold, biological response is influenced by surface roughness, homogeneity, and hydrophilicity.

Therefore, other than lack of sulfated polysaccharide species, cell behavior of PLA-REF sample is influenced by hydrophilic surface behavior, which affects cell attachment, as surface homogeneity and roughness are the same for each sample, which was confirmed by SEM micrographs. All fucoidan-loaded samples reached better cell proliferation compared to the reference PLA-REF sample. This behavior confirms the cytocompatibility of each fucoidan species. Moreover, lower surface hydrophilicity of the fucoidan loaded samples also contributed to cell adhesion performance. However, besides differences in the cell quantity also



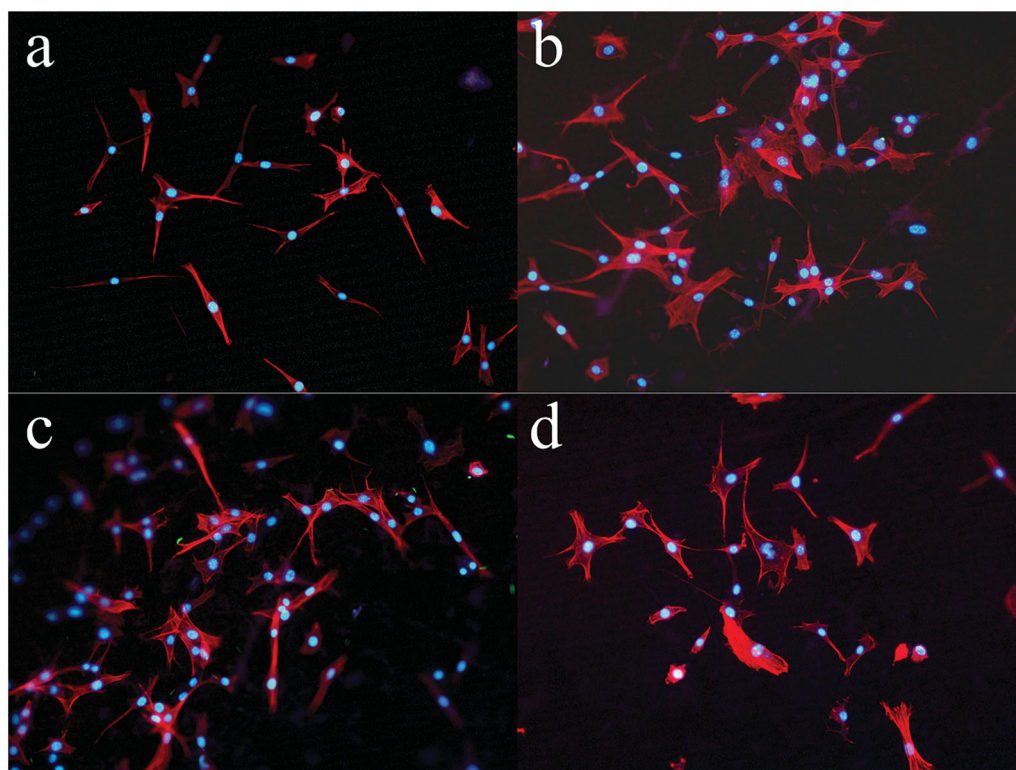


**Figure 4.** Morphology of NIH/3T3 fibroblast cells after 72 h: (a) PLA-REF. (b) PLA-RF-FV. (c) PLA-RF-MP. (d) PLA-RF-UP. The magnification is 100 $\times$ .

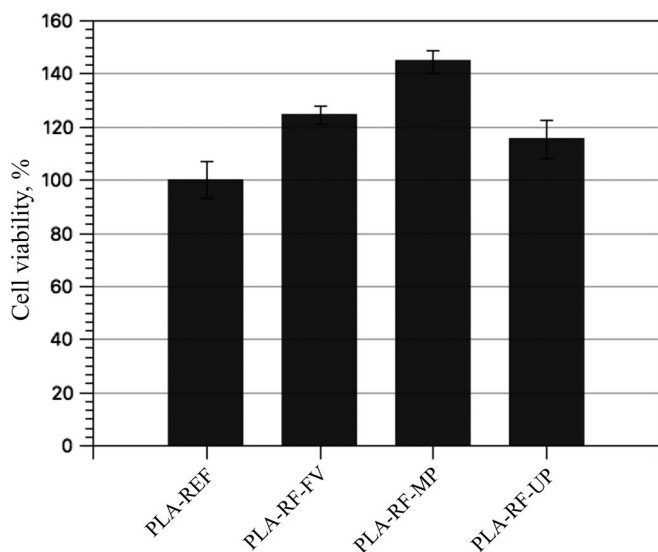


**Figure 5.** Cell viability of NIH/3T3 cells after 72 h on individual samples.

differences in cell morphology were observed on fucoidan-loaded samples. On samples PLA-RF-FV and PLA-RF-UP, the cells did not spread in typical elongated shapes. On the contrary, on sample PLA-RF-MP cell morphology is exactly fibroblast-like. Regarding the cell quantity, PLA-RF-MP exhibited the highest viability, followed by the PLA-RF-FV sample and the lowest cell viability is observed for the sample PLA-RF-UP, among the fucoidan-loaded samples. These results correspond to the SEM-EDS results, in that the level of the sulfate was observed in the same order.

These results correspond also with the results from cell viability. As can be seen in [Figure 5](#), the fucoidan loading

has a positive impact on cell viability. The viability was higher compared to the reference sample of PLA-REF in all fucoidan-loaded samples. The highest viability was observed on the sample PLA-RF-MP where it reached 144.5%, followed by 124.1% of PLA-RF-FV and 115.3% of PLA-RF-UP.

#### 4. Conclusion

The highly porous PLA scaffold was prepared by solution casting/porogen leaching technique with 25  $\mu\text{m}$  of thickness and pore sizes between 500 nm and 10  $\mu\text{m}$ . Three different sources of fucoidan from *Fucus vesiculosus*, *Macrocystis pyrifera*, and *Undaria pinnatifida* were successfully immobilized onto the highly porous PLA surface, after the activation of the surface by RF air plasma treatment, as it was provided by SEM-EDS data. Plasma treatment significantly increased the surface wettability of the PLA surface by decreasing the water contact angle values from 82.3 $^\circ$  to 58.3 $^\circ$ . The cytocompatibility assay was studied using mouse embryonic fibroblast cells (NIH/3T3) to compare cell proliferation on the fucoidan immobilized surfaces. It is demonstrated that PLA scaffold modified by plasma treatment and loaded with fucoidan can significantly increase fibroblast adhesion and proliferation. Among the samples studied, PLA-RF-MP demonstrated the morphology of fibroblast-like cells and had the highest cell viability.

#### Funding

This work was supported by the Ministry of Education, Youth and Sports of the Czech Republic [Program NPU I, LO1504] and Czech Science Foundation [Grant no. 19-16861S].

## ORCID

Kadir Ozaltın  <http://orcid.org/0000-0002-7619-5321>

## References

- [1] Silva, D.; Kaduri, M.; Poley, M.; Adir, O.; Krinsky, N.; Shainsky-Roitman, J.; Schroeder, A. Biocompatibility, Biodegradation and Excretion of Poly(lactic Acid) (PLA) in Medical Implants and Theranostic Systems. *Chem. Eng. J.* **2018**, *340*, 9–14.
- [2] Wood, A. T.; Everett, D.; Kumar, S.; Mishra, M. K.; Thomas, V. Fiber Length and Concentration: Synergistic Effect on Mechanical and Cellular Response in Wet-Laid Poly(lactic acid) Fibrous Scaffolds. *J. Biomed. Mater. Res. Part B Appl. Biomater.* **2019**, *107*, 332–341. DOI: [10.1002/jbm.b.34125](https://doi.org/10.1002/jbm.b.34125).
- [3] Qi, F.; Wu, J.; Li, H.; Ma, G. Recent Research and Development of PLGA/PLA Microspheres/Nanoparticles: A Review in Scientific and Industrial Aspects. *Front. Chem. Sci. Eng.* **2019**, *13*, 14–27. DOI: [10.1007/s11705-018-1729-4](https://doi.org/10.1007/s11705-018-1729-4).
- [4] Gomaa, S. F.; Madkour, T. M.; Moghannem, S.; El-Sherbiny, I. M. New Poly(lactic Acid)/Cellulose Acetate-Based Antimicrobial Interactive Single Dose Nanofibrous Wound Dressing Mats. *Int. J. Biol. Macromol.* **2017**, *105*, 1148–1160. DOI: [10.1016/j.ijbiomac.2017.07.145](https://doi.org/10.1016/j.ijbiomac.2017.07.145).
- [5] Chen, J.; Ye, J.; Liao, X.; Li, S.; Xiao, W.; Yang, Q.; Li, G. Organic Solvent Free Preparation of Porous Scaffolds Based on the Phase Morphology Control Using Supercritical CO<sub>2</sub>. *J. Supercrit. Fluid.* **2019**, *149*, 88–96. DOI: [10.1016/j.supflu.2019.03.021](https://doi.org/10.1016/j.supflu.2019.03.021).
- [6] Phaechamud, T.; Chitrattha, S. Pore Formation Mechanism of Porous Poly(DL-Lactic Acid) Matrix Membrane. *Mater. Sci. Eng. C Mater. Biol. Appl.* **2016**, *61*, 744–752. DOI: [10.1016/j.msec.2016.01.014](https://doi.org/10.1016/j.msec.2016.01.014).
- [7] Mosanenzadeh, S. G.; Naguib, H. E.; Park, C. B.; Atalla, N. Development of Poly(lactide) Open-Cell Foams with Bimodal Structure for High-Acoustic Absorption. *J. Appl. Polym. Sci.* **2014**, *131*, 1–11.
- [8] Chen, B. Y.; Wang, Y. S.; Mi, H. Y.; Yu, P.; Kuang, T. R.; Peng, X. F.; Wen, J. S. Effect of Poly(Ethylene Glycol) on the Properties and Foaming Behavior of Macroporous Poly(Lactic Acid)/Sodium Chloride Scaffold. *J. Appl. Polym. Sci.* **2014**, *131*, 41191. DOI: [10.1002/app.41181](https://doi.org/10.1002/app.41181).
- [9] Hollister, S. J. Porous Scaffold Design for Tissue Engineering. *Nat. Mater.* **2005**, *4*, 518–524. DOI: [10.1038/nmat1421](https://doi.org/10.1038/nmat1421).
- [10] Chitrattha, S.; Phaechamud, T. Porous Poly(DL-Lactic Acid) Matrix Film with Antimicrobial Activities for Wound Dressing Application. *Mater. Sci. Eng. C Mater. Biol. Appl.* **2016**, *58*, 1122–1130. DOI: [10.1016/j.msec.2015.09.083](https://doi.org/10.1016/j.msec.2015.09.083).
- [11] Lucke, A.; Tessmar, J.; Schnell, E.; Schmeer, G.; Göpferich, A. Biodegradable Poly(D,L-Lactic Acid)-Poly(Ethylene Glycol)-Monomethyl Ether Diblock Copolymers: structures and Surface Properties Relevant to Their Use as Biomaterials. *Biomaterials* **2000**, *21*, 2361–2370. DOI: [10.1016/S0142-9612\(00\)00103-4](https://doi.org/10.1016/S0142-9612(00)00103-4).
- [12] Zhong, T.; Jiao, Y.; Guo, L.; Ding, J.; Nie, Z.; Tan, L.; Huang, R. Investigations on Porous PLA Composite Scaffolds with Amphiphilic Block PLA-b-PEG to Enhance the Carrying Property for Hydrophilic Drugs of Excess Dose. *J. Appl. Polym. Sci.* **2017**, *134*, 44489–44496. DOI: [10.1002/app.44489](https://doi.org/10.1002/app.44489).
- [13] Rashmi, B. J.; Prashantha, K.; Lacrampe, M. F.; Krawczak, P. Toughening of Poly(Lactic Acid) without Sacrificing Stiffness and Strength by Melt-Blending with Polyamide 11 and Selective Localization of Halloysite Nanotubes. *Express Polym. Lett.* **2015**, *9*, 721–735. DOI: [10.3144/expresspolymlett.2015.67](https://doi.org/10.3144/expresspolymlett.2015.67).
- [14] Quiles-Carrillo, L.; Montanes, N.; Pineiro, F.; Jorda-Vilaplana, A.; Torres-Giner, S. Ductility and Toughness Improvement of Injection-Molded Compostable Pieces of Poly(lactide) by Melt Blending with Poly( $\epsilon$ -Caprolactone) and Thermoplastic Starch. *Materials* **2018**, *11*, 2138–2158. DOI: [10.3390/ma11112138](https://doi.org/10.3390/ma11112138).
- [15] Zhu, X.; Zhong, T.; Huang, R.; Wan, A. Preparation of Hydrophilic Poly(Lactic Acid) Tissue Engineering Scaffold via (PLA)-(PLA-b-PEG)-(PEG) Solution Casting and Thermal-Induced Surface Structural Transformation. *J. Biomater. Sci. Polym. Ed.* **2015**, *26*, 1286–1296. DOI: [10.1080/09205063.2015.1088125](https://doi.org/10.1080/09205063.2015.1088125).
- [16] Hamid, Z. A. A.; Tham, C. Y.; Ahmad, Z. Preparation and Optimization of Surface-Engineered Poly(Lactic Acid) Microspheres as a Drug Delivery Device. *J. Mater. Sci.* **2018**, *53*, 4745–4758. DOI: [10.1007/s10853-017-1840-9](https://doi.org/10.1007/s10853-017-1840-9).
- [17] Cheng, K. Y.; Chang, C. H.; Yang, Y. W.; Liao, G. C.; Liu, C. T.; Wu, J. S. Enhancement of Cell Growth on Honeycomb-Structured Poly(lactide) Surface Using Atmospheric-Pressure Plasma Jet Modification. *Appl. Surf. Sci.* **2017**, *394*, 534–542. DOI: [10.1016/j.apsusc.2016.10.093](https://doi.org/10.1016/j.apsusc.2016.10.093).
- [18] Jacobs, T.; Declercq, H.; Geyter, N. D.; Cornelissen, R.; Dubruel, P.; Leys, C.; Beaurain, A.; Payen, E.; Morent, R. Plasma Surface Modification of Poly(lactic Acid) to Promote Interaction with Fibroblasts. *J. Mater. Sci. Mater. Med.* **2013**, *24*, 469–478. DOI: [10.1007/s10856-012-4807-z](https://doi.org/10.1007/s10856-012-4807-z).
- [19] Wang, S.; Cui, W.; Bei, J. Bulk and Surface Modifications of Poly(lactide). *Anal. Bioanal. Chem.* **2005**, *381*, 547–556. DOI: [10.1007/s00216-004-2771-2](https://doi.org/10.1007/s00216-004-2771-2).
- [20] Stloukal, P.; Novák, I.; Mičušík, M.; Procházka, M.; Kucharczyk, P.; Chodák, I.; Lehocký, M.; Sedlářík, V. The Effect of Plasma Treatment on the Release Kinetics of a Chemotherapy Drug from Biodegradable Polyester Films and PolyesterUrethane Films. *Int. J. Polym. Mater.* **2018**, *67*, 161–173. DOI: [10.1080/00914037.2017.1309543](https://doi.org/10.1080/00914037.2017.1309543).
- [21] Fitton, J. H. Therapies from Fucoidan; Multifunctional Marine Polymers. *Mar. Drugs* **2011**, *9*, 1731–1760. DOI: [10.3390/md9101731](https://doi.org/10.3390/md9101731).
- [22] Ale, M. T.; Maruyama, H.; Tamauchi, H.; Mikkelsen, J. D.; Meyer, A. S. Fucoidan from Sargassum sp. and Fucus Vesiculosus Reduces Cell Viability of Lung Carcinoma and Melanoma Cells in Vitro and Activates Natural Killer Cells in Mice *In Vivo*. *Int. J. Biol. Macromol.* **2011**, *49*, 331–336. DOI: [10.1016/j.ijbiomac.2011.05.009](https://doi.org/10.1016/j.ijbiomac.2011.05.009).
- [23] Wu, L.; Sun, J.; Su, X.; Yu, Q.; Yu, Q.; Zhang, P. A Review About the Development of Fucoidan in Antitumor Activity: Progress and Challenges. *Carbohydr. Polym.* **2016**, *154*, 96–111. DOI: [10.1016/j.carbpol.2016.08.005](https://doi.org/10.1016/j.carbpol.2016.08.005).
- [24] Tengdelius, M.; Lee, C.-J.; Grenegård, M.; Griffith, M.; Pålsson, P.; Konradsson, P. Synthesis and Biological Evaluation of Fucoidan-Mimetic Glycopolymers Through Cyanoxyl-Mediated Free-Radical Polymerization. *Biomacromolecules* **2014**, *15*, 2359–2368. DOI: [10.1021/bm5002312](https://doi.org/10.1021/bm5002312).
- [25] Dore, C. M. P. G.; Alves, M. G. C. F.; Will, L. S. E. P.; Costa, T. G.; Sabry, D. A.; Rego, L. A. R. S.; Accardo, C. M.; Rocha, H. A. O.; Filgueira, L. G. A.; Leite, E. L. A Sulfated Polysaccharide, Fucans, Isolated from Brown Algae *Sargassum vulgare* with Anticoagulant, Antithrombotic, Antioxidant and Anti-Inflammatory Effects. *Carbohydr. Polym.* **2013**, *91*, 467–475. DOI: [10.1016/j.carbpol.2012.07.075](https://doi.org/10.1016/j.carbpol.2012.07.075).
- [26] Zhao, X.; Dong, S.; Wang, J.; Li, F.; Chen, A.; Li, B. A Comparative Study of Antithrombotic and Antiplatelet Activities of Different Fucoidans from *Laminaria japonica*. *Thromb. Res.* **2012**, *129*, 771–778. DOI: [10.1016/j.thromres.2011.07.041](https://doi.org/10.1016/j.thromres.2011.07.041).
- [27] Jin, W.; Zhang, Q.; Wang, J.; Zhang, W. A Comparative Study of the Anticoagulant Activities of Eleven Fucoidans. *Carbohydr. Polym.* **2013**, *91*, 1–6. DOI: [10.1016/j.carbpol.2012.07.067](https://doi.org/10.1016/j.carbpol.2012.07.067).
- [28] Wijesinghe, W. A. J. P.; Jeon, Y. J. Biological Activities and Potential Industrial Applications of Fucoose Rich Sulfated Polysaccharides and Fucoidans Isolated from Brown Seaweeds: A Review. *Carbohydr. Polym.* **2012**, *88*, 13–20. DOI: [10.1016/j.carbpol.2011.12.029](https://doi.org/10.1016/j.carbpol.2011.12.029).
- [29] Lu, K. Y.; Li, R.; Hsu, C. H.; Lin, C. W.; Chou, S. C.; Tsai, M. L.; Mi, F. L. Development of a New Type of Multifunctional

- Fucoidan-Based Nanoparticles for Anticancer Drug Delivery. *Carbohydr. Polym.* **2017**, *165*, 410–420. DOI: [10.1016/j.carbpol.2017.02.065](https://doi.org/10.1016/j.carbpol.2017.02.065).
- [30] Ozaltin, K.; Lehocky, M.; Humpolicek, P.; Pelkova, J.; Saha, P. A New Route of Fucoidan Immobilization on Low Density Polyethylene and Its Blood Compatibility and Anticoagulation Activity. *Int. J. Mol. Sci.* **2016**, *17*, 1–12.
- [31] Ozaltin, K.; Lehocky, M.; Humpolicek, P.; Pelkova, J.; Martino, A. D.; Karakurt, I.; Saha, P. Anticoagulant Polyethylene Terephthalate Surface by Plasma Mediated Fucoidan Immobilization. *Polymers* **2019**, *11*, 750. DOI: [10.3390/polym11050750](https://doi.org/10.3390/polym11050750).
- [32] Sarvari, R.; Sattari, S.; Massoumi, B.; Agbolaghi, S.; Beygi-Khosrowshahi, Y.; Kahaie-Khosrowshahi, A. Composite Electrospun Nanofibers of Reduced Graphene Oxide Grafted with Poly(3-Dodecylthiophene) and Poly(3-Thiophene Ethanol) and Blended with Polycaprolactone. *J. Biomater. Sci. Polym. Ed.* **2017**, *28*, 1740–1761. DOI: [10.1080/09205063.2017.1354167](https://doi.org/10.1080/09205063.2017.1354167).
- [33] Massoumi, B.; Sarvari, R.; Agbolaghi, S. Biodegradable and Conductive Hyperbranched Terpolymers Based on Aliphatic Polyester, Poly(D,L-Lactide), and Polyaniline Used as Scaffold in Tissue Engineering. *Int. J. Polym. Mater.* **2018**, *67*, 808–821. DOI: [10.1080/00914037.2017.1383248](https://doi.org/10.1080/00914037.2017.1383248).
- [34] Sarvari, R.; Akbari-Alanjaraghi, M.; Massoumi, B.; Beygi-Khosrowshahi, Y.; Agbolaghi, S. Conductive and Biodegradable Scaffolds Based on a Five-Arm and Functionalized Star-like Polyaniline–Polycaprolactone Copolymer with a d-Glucose Core. *New J. Chem.* **2017**, *41*, 6371–6384. DOI: [10.1039/C7NJ01063J](https://doi.org/10.1039/C7NJ01063J).
- [35] Hatamzadeh, M.; Sarvari, R.; Massoumi, B.; Agbolaghi, S.; Samadian, F. Liver Tissue Engineering via Hyperbranched Polypyrrole Scaffolds. *Int. J. Polym. Mater. Po.* **2019**, *68*, 1–11. DOI: [10.1080/00914037.2019.1667800](https://doi.org/10.1080/00914037.2019.1667800).
- [36] Sarvari, R.; Agbolaghi, S.; Beygi-Khosrowshahi, Y.; Massoumi, B.; Bahadori, A. 3D Scaffold Designing Based on Conductive/Degradable Tetrapolymeric Nanofibers of PHEMA-co-PNIPAAm-co-PCL/PANI for Bone Tissue Engineering. *J. Ultrafine Grained Nanostruct. Mater.* **2018**, *51*, 101–114.
- [37] Sarvari, R.; Agbolaghi, S.; Beygi-Khosrowshahi, Y.; Massoumi, B. Towards Skin Tissue Engineering Using Poly(2-Hydroxy Ethyl Methacrylate)-co-Poly(N-Isopropylacrylamide)-co-Poly( $\epsilon$ -Caprolactone) Hydrophilic Terpolymers. *Int. J. Polym. Mater.* **2019**, *68*, 691–700. DOI: [10.1080/00914037.2018.1493682](https://doi.org/10.1080/00914037.2018.1493682).
- [38] Sarvari, R.; Massoumi, B.; Zareh, A.; Beygi-Khosrowshahi, Y.; Agbolaghi, S. Porous Conductive and Biocompatible Scaffolds on the Basis of Polycaprolactone and Polythiophene for Scaffolding. *Polym. Bull.* **2020**, *77*, 1829–1846. DOI: [10.1007/s00289-019-02732-z](https://doi.org/10.1007/s00289-019-02732-z).
- [39] Massoumi, B.; Sarvari, R.; Zareh, A.; Beygi-Khosrowshahi, Y.; Agbolaghi, S. Polyanizidine and Polycaprolactone Nanofibers for Designing the Conductive Scaffolds. *Fibers Polym.* **2018**, *19*, 2157. DOI: [10.1007/s12221-018-8233-9](https://doi.org/10.1007/s12221-018-8233-9).
- [40] Saha, D.; Samal, S. K.; Biswal, M.; Mohanty, S.; Nayak, S. K. Preparation and Characterization of Poly(Lactic Acid)/Poly(Ethylene Oxide) Blend Film: Effects of Poly(Ethylene Oxide) and Poly(Ethylene Glycol) on the Properties. *Polym. Int.* **2019**, *68*, 164–172. DOI: [10.1002/pi.5718](https://doi.org/10.1002/pi.5718).
- [41] Moradkhannejhad, L.; Abdouss, M.; Nikfarjam, N.; Mazinani, S.; Sayar, P. Electrospun Curcumin Loaded Poly(Lactic Acid) Nanofiber Mat on the Flexible Crosslinked PVA/PEG Membrane Film: Characterization and *In Vitro* Release Kinetic Study. *Fibers Polym.* **2017**, *18*, 2349–2360. DOI: [10.1007/s12221-017-7543-7](https://doi.org/10.1007/s12221-017-7543-7).
- [42] Tserepi, A.; Gogolides, E.; Bourkoula, A.; Kanioura, A.; Kokkoris, G.; Petrou, P. S.; Kakabakos, S. E. Plasma Nanotextured Polymeric Surfaces for Controlling Cell Attachment and Proliferation: A Short Review. *Plasma Chem. Plasma Process.* **2016**, *36*, 107–120. DOI: [10.1007/s11090-015-9674-1](https://doi.org/10.1007/s11090-015-9674-1).
- [43] Winthrop, C. *New Developments in Poly(lactic Acid) Research*; Nova Science Publishers: New York, 2015.